

(R)-(+)- α -Methylvaline Raman/IR Spectroscopic and DFT Dimer Analysis

Shashikala Yalagi

Department of Studies in Physics

Davangere University, Davangere – 577007, Karnataka, India

Abstract:- Raman and IR spectral measurements in the 3500 – 400 cm^{-1} have been carried out for the solid sample of (R)-(+)- α -Methylvaline. The spectral features indicated that the molecule is a zwitterion, as is true of amino acids, and is involved in H-bonding, namely, intermolecular $\text{N-H}\cdots\text{O}$ bonding. To account for these aspects, we have determined a zwitterionic stable monomer structure in water as a solvent at B3LYP/6-311++G(d,p) level, and from this monomer, a dimer species with $\text{N-H}\cdots\text{O}$ bonding is constructed. On the basis of NBO analysis, it has been shown that the delocalization of electron densities between lone pair (LP) of Oxygen with the anti-bonding (σ^*) orbital of N-H moiety is consistent with the geometrical structure of the dimer. Molecular electrostatic potentials have been used to demonstrate intermolecular donor (O) – acceptor (N-H) interaction. Predicted deformation modes for N-H_3^+ and CO_2^- are in fair agreement with measured frequencies than stretching modes.

Keywords:- (R)-(+)- α -Methylvaline; IR; Raman; DFT; $\text{N-H}\cdots\text{O}$ Bonding.

I. INTRODUCTION

Amino acids, peptides and proteins have been the subject of spectroscopic investigations for a long time [1]. IR and Raman investigations of several amino acids in the solid and liquid forms have established the ZW structure [2-3]. All the 20 naturally occurring amino acids are α -amino acids and used by cells to synthesize proteins. Valine has both a primary amino group and a primary carboxyl group. The carboxyl group of valine donates its proton to the amino group that results in zwitterionic (ZW) structure in solid and liquid state. These zwitterions create H-bonds in the form of $\text{N-H}\cdots\text{O}-\text{C}$, which are very strong bonds [4-5]. (R)-(+)- α -Methylvaline ($\text{C}_6\text{H}_{13}\text{NO}_2$), being a methyl derivative of natural amino acid – Valine, is an unnatural α -amino acid. It is utilized, among others, as a chiral building block in asymmetric synthesis.

Several spectroscopic and theoretical studies have been devoted to understand the role of amino acids in physiological and chemical processes. The neutron scattering study reported that L-valine crystallizes in a monoclinic structure, with $P2_1$ space group having four molecules per unit cell and $\text{N-H}\cdots\text{O}$ bond connecting the amine and carboxyl groups of neighbouring valine molecules [3, 6-7]. IR and Raman spectral studies have been made by Krishnan et al. and others for natural amino acids including L-valine in ZW form showed that the N-H stretching frequencies are influenced

by H-bonding and characteristic lines due to N-H_3^+ and CO_2^- groups have been identified in Raman spectrum [8]. Inelastic Incoherent Neutron Scattering (IINS) studies along with IR and Raman spectral studies on L- and DL-valine is also helpful in understanding vibrations due to out of plane $\text{N-H}\cdots\text{O}$ bonding at 279, 505 and 513 cm^{-1} [3, 9]. To aid the vibrational analysis, DFT calculations have been carried out for optimization and for simulation of IR and Raman spectra for the DL-valine zwitterion [10]. Calculations have also been carried out for the non-zwitterionic form of L-valine which include simulation of IR, Raman, ^{13}C and ^1H NMR spectra to aid the experimental spectra, HOMO-LUMO energy gap to show the charge transfer within the monomer and molecular electrostatic potential (MEP) mapping to know the nature of chemical bond [4]. With this background, in the present paper we present the FT-IR and Raman spectroscopic study of (R)-(+)- α -Methylvaline (methyl derivative of valine) aided by DFT calculations.

The experimental IR spectrum with broad absorptions near 3100 cm^{-1} and combinations near 2710 – 2050 cm^{-1} , as characteristic modes of amino acids, have motivated us to construct a dimer model with $\text{N-H}\cdots\text{O}$ bonding between N-H_3^+ and CO_2^- moieties. To account for experimental spectra, we modeled ZW monomer and dimer for (R)-(+)- α -Methylvaline in water at B3LYP/6-311++G(d,p) level. The proposed model explains strongly characteristic IR and Raman modes observed near 3160 – 2000 cm^{-1} and 1650 – 990 cm^{-1} and it satisfactorily approximates to its ZW form in the solid phase of the sample. The H-bonding is interpreted in terms of delocalization of electron densities between lone pair of oxygen (O) and N-H anti-bonding orbitals and electrostatic potentials over the donor-acceptor interaction.

II. EXPERIMENTAL AND COMPUTATIONAL DETAILS

➤ Experimental

The solid sample of (R)-(+)- α -Methylvaline was used as received (Aldrich Chemical Co). The IR spectral measurements were carried out on the Nicolet 6700 FT-IR spectrometer. The spectrometer consisted of an Alum standard ETC Ever-Glo IR source and the signals were collected by Deuterated Triglycine Sulphate (DTGS) detector with KBr window. The sample preparation was made using KBr pellete technique and the spectra were recorded in the region 4000 – 400 cm^{-1} for 50 scans with the resolution of 4 cm^{-1} . The Raman spectra (4000 – 400 cm^{-1}) were recorded on the Nicolet NXR-FT-Raman spectrometer. The spectrometer consisted of a Nd:YVO₄ (1064 nm) laser as an excitation source, CaF₂ beam splitter and a high-performance LN₂

cooled Ge detector. Solid sample is taken in a glass tube and the spectrum is recorded. A total of 500 numbers of scans were taken for each spectral measurement with the resolution of 4 cm^{-1} .

➤ Computational

The electronic structure calculations have been performed using DFT methods in the *Gaussian 09W* and *GaussView5* programs [11-12]. The levels used for calculation include RHF/3-21G and B3LYP/6-311++G(d, p) [13]. The molecular structure of (R)-(+)- α -Methylvaline (RMV) is shown in Fig. 1(a). As a first step in modeling, we searched for all possible conformers in neutral (NE) form of RMV (refer Fig. 1(a)) by performing a relaxed potential energy surface (PES) scan at RHF/3-21G level of theory. To confirm the orientation of methyl groups with respect to the rest of the molecule, PES scan performed by varying the dihedral angle τ_1 from 0° to 180° at 10° interval. This scan produced a minimum at 180° . Further, the dihedral angles τ_2

(H-O-C-C) and τ_3 (H-N-C-C) were varied simultaneously at 10° interval. Optimization of all the minimum energy points was carried out by performing frequency analysis at B3LYP/6-311++G(d,p) level which yielded a single structure in NE form. The optimized NE structure is further optimized into its ZW using self-consistent reaction field solvation model based on charge density (SCRF-SMD) implicit solvation methods at DFT B3LYP/6-311++G(d,p) level and the optimized ZW is shown in Fig. 1(b). The experimental absorption spectrum (Fig. 2) in the region $3500 - 2000\text{ cm}^{-1}$ indicates the strong H-bonding. Thus to understand H-bonding behaviour and its influence on the vibrational spectra, we modeled ZW dimer through $-N-H\cdots O$ bonding using two ZW monomers at DFT B3LYP/6-311++G(d,p) level. The vibrational modes are characterized in terms of potential energy distributions (PED) that were calculated using VEDA program [14].

III. RESULTS AND DISCUSSION

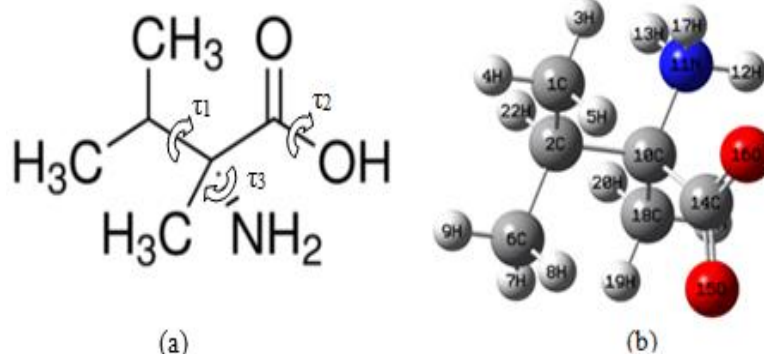


Fig 1 (a) Molecular Structure of (R)- (+)- α -Methylvaline Showing The Dihedral Angles τ_1 , τ_2 And τ_3 for the Determination of Stable Conformers. (b) Optimized Zwitterionic Structure of (R)-(+)- α -Methylvaline.

Experimental FT-IR and Raman spectra of solid sample of (R)-(+)- α -Methylvaline are presented in Fig. 2. The optimization and frequency calculations of the ZW dimer were carried out. The optimized dimer structure is presented in Fig. 3 and the hydrogen bonding parameters of ZW dimer are presented in Table 1. From table 1, we note that the N-H bond length in dimer showing the elongation of bond in dimer by 3%. The angle between N-H and $H\cdots O$ being 175.1° . The $H\cdots O$ bond distance 1.744 \AA being shorter than the sum of their respective van der Waal's radii (2.72 \AA) and the $N\cdots O$ distance 2.796 \AA suggesting a strong H-bonding [15].

➤ Vibrational Analysis

Experimental FT-IR and Raman spectra are shown in Fig. 2. We present the simulated ZW monomer and dimer IR spectra along with that experimental IR spectrum in Fig. 4. Likewise the simulated monomer and dimer Raman spectra along with that of experimental Raman spectrum of RMV are shown in Fig. 5. Experimental IR spectrum is marked by the medium weak broad absorption band in $3500 - 2000\text{ cm}^{-1}$

region, very strong to medium bands in $1600 - 1300\text{ cm}^{-1}$ region and weak bands in lower frequency region. On the other hand, Raman spectrum is marked by a series of strong bands in $3000 - 2800\text{ cm}^{-1}$ region, medium to weak bands in $1600 - 400\text{ cm}^{-1}$ region. A detailed assignments of simulated monomer, dimer vibrational bands with that of experimental FT-IR and Raman bands are presented in Table. 2.

Table 1 Hydrogen Bonding Parameters of Zwitterionic RMV Dimer.

Parameters	RMV
N18-H20	1.052 \AA
H20 \cdots O48	1.744 \AA
N18 \cdots O48	2.796 \AA
N18-H20 \cdots O48	175.1°

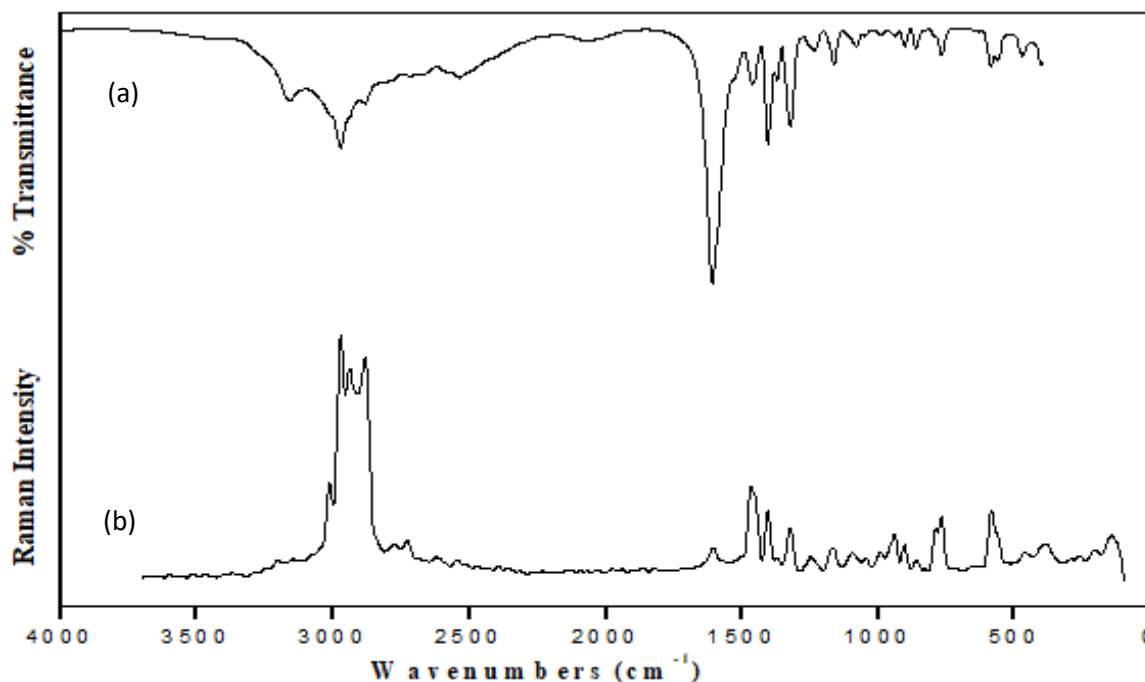


Fig 2 Experimental (a) FT-IR And (b) Raman Spectra of Solid Sample of (R)-(+)- α -Methylvaline

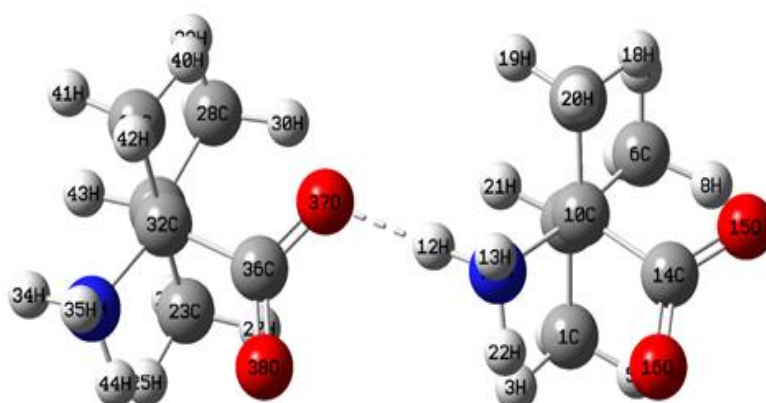


Fig 3 Optimized Zwitterionic Structure of (R)-(+)- α -Methylvaline Dimer

For a given dimer, there are two pairs of -NH_3^+ and -CO_2^- groups one pair on each monomer, of which, -NH_3^+ group of one monomer and -CO_2^- group of other monomer (conjugate pair – I) form the intermolecular H-bonding. The modes due to these bonded functional groups are referred to as bonded modes whose frequencies are close to experimental frequencies. Free modes refer to the vibrations due to other conjugate pair of -NH_3^+ and -CO_2^- groups (conjugate pair – II) which are not involved in $\text{-N-H}\cdots\text{O}$ bonding and the frequency values of free modes are very close to simulated monomer frequency values.

➤ NH_3^+ Vibrations

Amino acids are characterized by strong absorption between $3200 - 3000 \text{ cm}^{-1}$ due to asymmetric and symmetric -NH_3^+ stretching and the asymmetric and symmetric deformation modes are expected to fall in the region $1660 - 1600 \text{ cm}^{-1}$ and $1550 - 1485 \text{ cm}^{-1}$ [16]. For RMV four bands are predicted for stretching vibrations of -NH_3^+ group. The predicted band at 3384 cm^{-1} in dimer which is

correlated to the band at 3391 cm^{-1} in monomer is due to asymmetric stretching vibration of -NH_3^+ moiety. There is another predicted band due to -NH_3^+ asymmetric stretch at 3375 cm^{-1} in dimer being correlated to the band at 3367 cm^{-1} in monomer. This mode is identified as a medium weak broad IR absorption at 3162 cm^{-1} . The medium weak Raman band at 3013 cm^{-1} is assigned to symmetric stretching vibration of -NH_3^+ moiety and is predicted at 3302 cm^{-1} (3295 cm^{-1} in monomer). Another band at 2827 cm^{-1} predicted only in dimer due to symmetric stretching vibration which is downshifted from its usual absorption region due to $\text{-N-H}\cdots\text{O}$ bonding and is correlated against the observed weak Raman band at 2774 cm^{-1} . As for bending vibrations, three modes due to asymmetric and one mode due to symmetric bending are predicted. The band at 1587 cm^{-1} in dimer is correlated against the very strong absorption at 1610 cm^{-1} and is assigned to the bonded asymmetric bending mode of -NH_3^+ . Its Raman counterpart is weak band at 1606 cm^{-1} . The free asymmetric mode is predicted at 1573 cm^{-1} in dimer and at 1580 cm^{-1} in monomer. Another band is predicted at 1564

cm^{-1} in dimer due to bonded $-\text{NH}_3^+$ asymmetric bending and its free mode is predicted at 1533 cm^{-1} being correlated to the monomer mode at 1534 cm^{-1} . This mode is not observed either in IR or in Raman spectrum. The third band is computed only in dimer due to asymmetric bending at 1471 cm^{-1} is a coupled vibration with asymmetric stretching vibration of $-\text{CO}_2^-$. The symmetric bending mode is predicted at 1426 cm^{-1} in dimer and at 1409 cm^{-1} in monomer. This mode is identified as a strong IR absorption at 1405 cm^{-1} and medium weak Raman band at 1406 cm^{-1} . Two weak to medium bands observed at 990 cm^{-1} (986 cm^{-1} in Raman) and 862 cm^{-1} (860 cm^{-1} in Raman) are assigned to rocking modes of $-\text{NH}_3^+$ moiety correlated against the computed bands at 1020 cm^{-1} and 863 cm^{-1} respectively. Another band due to rocking vibration is predicted at 956 cm^{-1} as a coupled vibration with C-C stretching.

➤ CO_2^- Vibrations

Carboxylate group (CO_2^-) has two strongly coupled CO bonds with bond strengths intermediate between C-O and C=O bonds. This group absorbs strongly at $1600 - 1560 \text{ cm}^{-1}$ and weakly at 1410 cm^{-1} . In the present case, the observed band with medium intensity at 1462 cm^{-1} in IR spectrum and medium strong Raman band at 1466 cm^{-1} are assigned to asymmetric stretching vibration of $-\text{CO}_2^-$ group and is correlated against the predicted band in dimer at 1494 cm^{-1} for bonded vibration. Its free mode is predicted at 1502 cm^{-1} having same value in monomer. The $-\text{CO}_2^-$ symmetric stretching vibrations fall in the CH_3 bending region, so it

cannot be assigned unambiguously [17]. The symmetric stretching mode is predicted as a coupled vibration with CH_3 deformation at 1378 cm^{-1} . This mode is observed as a medium weak absorption at 1370 cm^{-1} . Another band at 1290 cm^{-1} predicted as symmetric stretching vibration and is correlated to the strong absorption at 1319 cm^{-1} and medium weak Raman band at 1322 cm^{-1} . These wavenumbers of $-\text{CO}_2^-$ stretching mode have shifted towards the lower frequency region due to the involvement of $-\text{CO}_2^-$ group in H-bonding. Weak to medium absorptions at 792 , 766 and 587 cm^{-1} are assigned to deformation vibrations of $-\text{CO}_2^-$ group and are predicted at 830 , 760 and 556 cm^{-1} respectively.

In addition to the stretching and bending frequencies of $-\text{NH}_3^+$ and $-\text{CO}_2^-$ groups, there appear a series of bands in the region $2700 - 2000 \text{ cm}^{-1}$ as a substructure on the broad absorption in the experimental IR spectrum. These bands are attributed to the combination of asymmetric bending vibration of $-\text{NH}_3^+$ moiety with the CN stretching or $-\text{NH}_3^+$ torsional modes [17-18]. In the present case, the medium absorptions at 2719 and 2685 cm^{-1} are due to $-\text{N}-\text{H}\cdots\text{O}$ bonding. The weak absorption band at 2066 cm^{-1} is assigned to the combination of asymmetric bending of $-\text{NH}_3^+$ (1610 cm^{-1}) and bending vibration of CN (471 cm^{-1}), the appearance of this mode indicates the existence of charged $-\text{NH}_3^+$ moiety. The weak absorption bands at 2579 and 2537 cm^{-1} are assigned to the combination of asymmetric bending and rocking vibration of $-\text{NH}_3^+$ group.

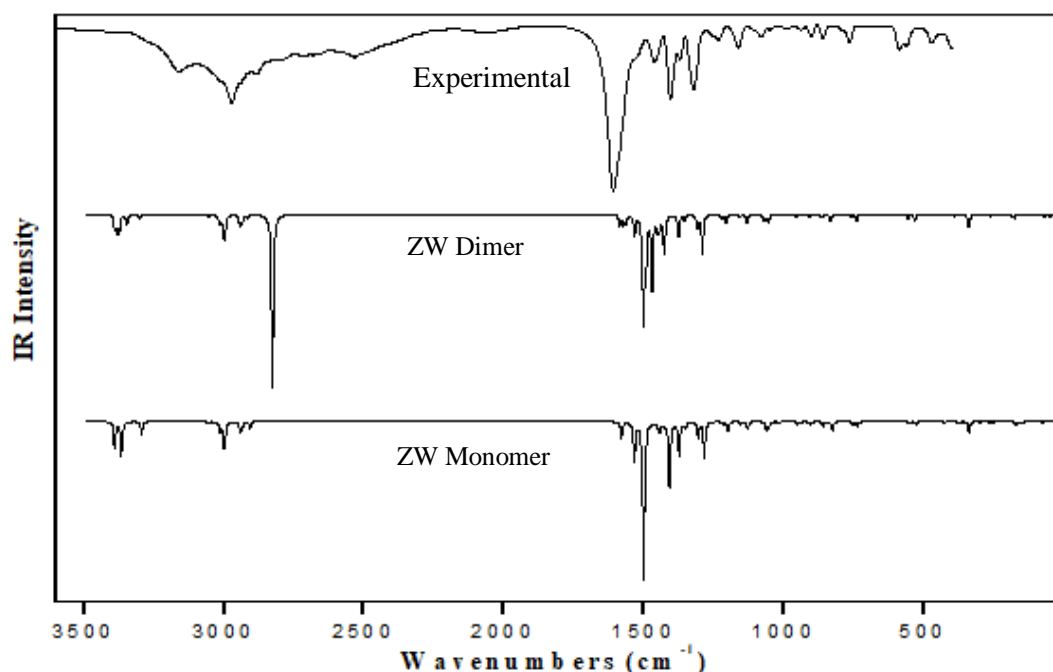


Fig 4 Experimental IR Spectrum Compared with ZW Monomer and Dimer Spectra of (R)-(+)- α -Methylvaline.

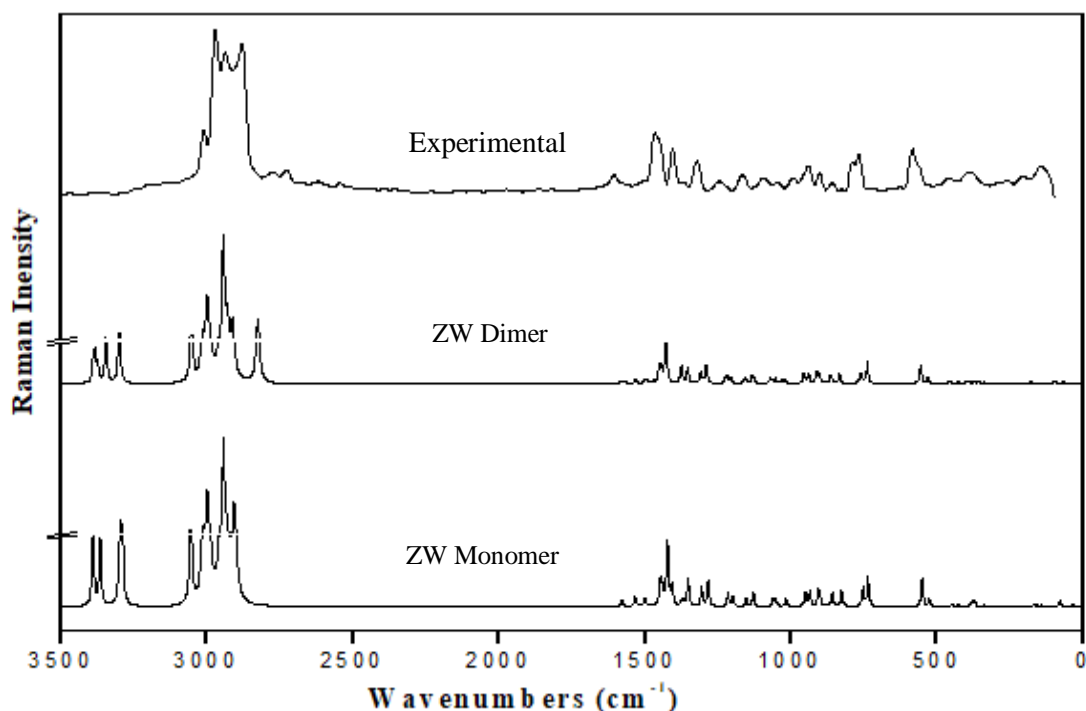


Fig 5 Experimental Raman Spectrum Compared with ZW Monomer and Dimer Spectra of (R)-(+)- α -Methylvaline. Ordinate in Simulated Spectra is Broken to Adjust the Bands from Overshooting Because of their Intensity.

➤ CH vibrations

The vibrations due to CH_3 and CH groups, which are uninfluenced by $-\text{N}-\text{H}\cdots\text{O}$ bonding show strong bands in Raman and IR spectra. The region $3000 - 2800 \text{ cm}^{-1}$ in Raman spectrum is marked by the series of CH_3 and CH vibrations [19]. These vibrations are strongest Raman bands in RMV. Since the molecule has three CH_3 groups, the computed spectra predict a series of stretching and deformation modes corresponding to these groups. The predicted bands are in good agreement with the experiment, though not all bands are observed. A very strong Raman mode at 2972 cm^{-1} is assigned to CH_3 asymmetric stretching and is computed at 2998 cm^{-1} . Its corresponding IR absorption is a strong band at 2973 cm^{-1} . Another very strong band in Raman at 2940 cm^{-1} is also assigned to CH_3 asymmetric stretching mode which is predicted accurately at 2947 cm^{-1} . The symmetric stretching mode is identified as a medium weak absorption in IR at 2882 cm^{-1} being correlated to the predicted band at 2937 cm^{-1} . Its Raman counterpart is a very strong band at 2882 cm^{-1} . The CH stretching mode is predicted at 2915 cm^{-1} . The predicted

spectra show a series of bands corresponding to CH_3 asymmetric bending at $1453, 1448, 1444, 1432, 1429$ and 1427 cm^{-1} and symmetric bending at $1378, 1357$ and 1353 cm^{-1} . CH bending vibration mode is predicted at 1351 and 1349 cm^{-1} . Coupled vibrations of skeletal CC stretching and bending, CN bending have appeared in $1250 - 1050 \text{ cm}^{-1}$. Two weak bands observed in IR at 1161 and 1085 cm^{-1} are assigned to the coupled vibration of CC stretching and bending vibrations. These modes are predicted at 1156 and 1065 cm^{-1} respectively. A coupled mode of CC and CN deformation is observed at 1050 (IR) and 1045 (Raman) cm^{-1} . The two predicted bands at 940 and 912 cm^{-1} are assigned to purely CC skeletal vibrations, of which the former mode is observed both in IR and Raman spectra as a medium weak band at 940 cm^{-1} . The weak absorptions at 471 and 401 cm^{-1} are assigned to CN bending. The vibrations below 400 cm^{-1} are due to torsional modes of CC, CN, CO. These modes are due to lattice vibrations of the molecule.

Table 2 Comparison of Experimental IR and Raman Vibrational Frequencies (Cm^{-1}) with Zwitterionic Monomer, Dimer Frequencies of (R)-(+)- α -Methylvaline with Assignments

Observed Frequencies		Computed Frequencies		Assignments
IR	Raman	Monomer	Dimer	
--	--	3391	3384	$\nu_{as}(\text{NH}_3^+, 100)$
3162 mw	--	3367	3375	$\nu_{as}(\text{NH}_3^+, 100)$
--	3013 mw	3295	3302	$\nu_s(\text{NH}_3^+, 100)$
--	--	3057	3058	$\nu_{as}(\text{CH}_3, 89)$
--	--	3015	3015	$\nu_{as}(\text{CH}_3, 97)$
--	--	3001	3004	$\nu_{as}(\text{CH}_3, 99)$
--	--	3000	3003	$\nu_{as}(\text{CH}_3, 97)$
--	--	2997	2999	$\nu_{as}(\text{CH}_3, 93)$
2973 s	2972 vs	2996	2998	$\nu_{as}(\text{CH}_3, 85)$
--	2940 vs	2945	2947	$\nu_{as}(\text{CH}_3, 92)$
--	--	2943	2944	$\nu_{as}(\text{CH}_3, 93)$
2882 mw	2882 vs	2935	2937	$\nu_s(\text{CH}_3, 91)$
--	--	2907	2915	$\nu(\text{CH}, 98)$
--	2774 w	--	2827	$\nu_s(\text{NH}_3^+, 94)$
2719 w	2728 w	--	--	1610 + 1050 (N-H...O bonding)
2685 w	--	--	--	1610 + 1050 (N-H...O bonding)
2579 w	--	--	--	1610 ($\beta_{as}(\text{NH}_3^+)$) + 990 ($\beta_r(\text{NH}_3^+)$)
2537 w	--	--	--	1610 ($\beta_{as}(\text{NH}_3^+)$) + 862 ($\beta_r(\text{NH}_3^+)$)
2066 w	--	--	--	1610 ($\beta_{as}(\text{NH}_3^+)$) + 471 ($\beta(\text{CN})$)
1610 vs	1606 w	--	1587 (b)	$\beta_{as}(\text{NH}_3^+, 90)$
--	--	1580	1573 (f)	
--	--	--	1564 (b)	$\beta_{as}(\text{NH}_3^+, 80)$
--	--	1534	1533 (f)	
1462 mw	1466 ms	1501	1502 (f)	$\nu_{as}(\text{CO}_2^-, 81)$
--	--	--	1494 (b)	
--	--	--	1471	$\beta_{as}(\text{NH}_3^+, 35), \nu_{as}(\text{CO}_2^-, 17)$
--	--	1451	1453	$\beta_{as}(\text{CH}_3, 81)$
--	--	1445	1448	$\beta_{as}(\text{CH}_3, 82)$
--	--	1441	1444	$\beta_{as}(\text{CH}_3, 64)$
--	--	1428	1432	$\beta_{as}(\text{CH}_3, 89)$
--	--	1424	1429	$\beta_{as}(\text{CH}_3, 63)$
--	--	1422	1427	$\beta_{as}(\text{CH}_3, 80)$

1405 s	1406 mw	1409	1426	β_s (NH ₃ ⁺ , 60), β_{as} (CH ₃ , 26)
1370 mw	--	--	1378	ν_s (CO ₂ ⁻ , 28), β_{as} (CH ₃ , 22)
--	--	1375	1378	β_s (CH ₃ , 61)
--	--	1368	1357	β_s (CH ₃ , 72)
--	--	1352	1353	β_s (CH ₃ , 55), β (CC, 18)
--	--	1351	--	β (CH, 57)
--	--	1349	1351	β (CH, 56), β (CN, 22)
1319 s	1322 mw	1284	1290	ν_s (CO ₂ ⁻ , 37), β (CH, 37)
1235 w	1246 w	1217	1219	β (CN, 21), ν (CC, 18)
--	--	1199	1205	β (CN, 27), ν (CC, 12)
1161 w	1167 w	1153	1156	β (CC, 32), ν (CC, 11)
--	--	1129	1130	β (CC, 20), β (CN, 12), ν (CC, 11)
1085 w	1096 w	1063	1065	β (CC, 12), ν (CC, 10)
1050 vw	1045 vw	1054	1055	β (CN, 16), β (CC, 13)
990 vw	986 vw	1017	1020	β_r (NH ₃ ⁺ , 44)
--	--	951	956	β_r (NH ₃ ⁺ , 28), ν (CC, 25)
940 vw	940 mw	936	940	ν (CC, 21), β (CC, 12)
--	--	908	912	β (CC, 17), ν (CC, 15)
903 w	904 mw	902	904	β (CC, 40)
862 w	860 vw	859	863	β_r (NH ₃ ⁺ , 26), ν (CC, 17)
792 w	797 w	827	830	β (CO ₂ ⁻ , 59), ν (CC, 15)
766 w	768 mw	755	760	β (CO ₂ ⁻ , 55), ν (CN, 17), ν (CC, 14)
--	--	736	739	β (CO ₂ ⁻ , 27), ν (CC, 21)
587 w	587 mw	551	556	β (CO ₂ ⁻ , 44), ν (CC, 14)
--	--	527	532	β (CO, 32), ν (CN, 22), β (CN, 11)
471 w	473 w	450	455	β (CN, 33), ν (CC, 11)
--	--	425	426	β (CC, 24), β (CN, 22)
Note: ν = stretching; β = bending; τ = torsional vibrations; <i>as</i> = antisymmetric; <i>s</i> = symmetric; <i>r</i> = rocking.				

➤ NBO Analysis:

NBO analysis was performed at B3LYP/6-311++G(d,p) level for the ZW monomer and dimer of RMV using NBO version 3.1 implemented in the Gaussian 09. The second order perturbation energies ($E^{(2)}$) were computed for dimer. The larger values of $E^{(2)}$ reflect the intensive interaction between donor and acceptor. The second order perturbation energies ($E^{(2)}$) for the orbital overlap between lone pair (*n*) of oxygen (O37) with the antibonding (σ^*) orbital of N-H (N11-H12).

The most important intermolecular interactions related to the dimer are from n_1 (O37), n_2 (O37) and n_3 (O37) with the antibonding N11-H12 orbital and amounts to the stabilization energies of 5.92, 20.52 and 0.19 Kcal/mol respectively. For the dimer, the graphical electron density maps of NBOs corresponding to these interactions are presented in Fig. 6 and the intermolecular interactions between some of the important donor-acceptor NBO pairs are presented in Table 3.

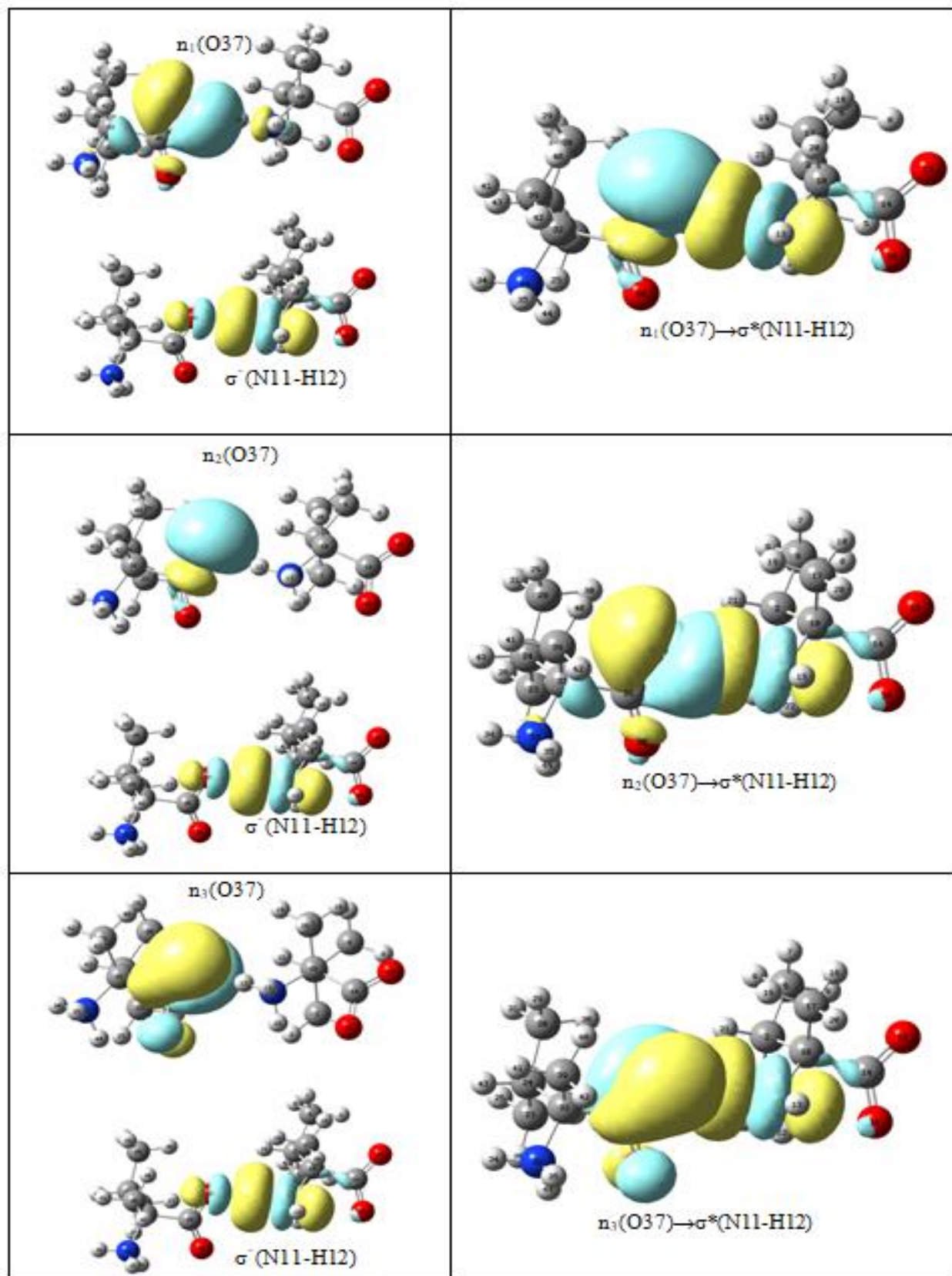


Fig 6 Electron Density Maps of Selected NBOs Involved in $-N-H \cdots O$ Bonding in Dimer

Note: Donor (lone pair orbital of O37) and acceptor (sigma antibonding orbital of N11–H12) NBOs are shown separately in left column and their overlapping due to H-bonding is shown in right column. Green and yellow colours of the orbitals correspond to positive and negative signs respectively.

Table 3 Computed Mixing Coefficients (λ), Charge Transfer (Q) Giving NBOs with Stabilization Energy Corresponding to $-N-H\cdots O$ Interaction in Dimer

NBOs $\Omega_i \rightarrow \Omega_j^*$	Mixing coefficient $\lambda_{i \rightarrow j}$	Charge transfer $Q_{i \rightarrow j}$	$E^{(2)a}$ kcal/mol
$n_1(O37) \rightarrow \sigma^*(N11-H12)$	0.0682	0.00932	5.92
$n_2(O37) \rightarrow \sigma^*(N11-H12)$	0.1582	0.05006	20.52
$n_3(O37) \rightarrow \sigma^*(N11-H12)$	0.0166	0.00055	0.19
$CR(O37) \rightarrow \sigma^*(N11-H12)$	0.0034	0.00002	0.28
$\sigma(C36-O37) \rightarrow \sigma^*(N11-H12)$	0.0116	0.00027	0.23

Note: Ω_i, Ω_j^* = donor, acceptor NBOs, σ^* = antibonding orbital, n = lone pair on oxygen atom, CR = core, ^aEnergy of hyperconjugative interaction (stabilization energy).

IV. CONCLUSIONS

FT-IR and Raman spectral measurements in the 3500 – 400 cm^{-1} have been carried out for the solid sample of (R)-(+)- α -Methylvaline. The spectral features indicated that the molecule is a zwitterion, as is true of amino acids, and is involved in H-bonding, namely, intermolecular $-N-H\cdots O$ bonding. To account for these aspects, we have determined a zwitterionic stable monomer structure in water medium at B3LYP/6-311++G(d,p) level, and from this monomer, a dimer species with $-N-H\cdots O$ bonding is constructed. The computed dimer spectra satisfactorily account for the bands in experimental spectra. On the basis of NBO analysis, it has been shown that the delocalization of electron densities between lone pair of oxygen with the anti-bonding orbital of N-H moiety is consistent with the geometrical structure of the dimer.

REFERENCES

- [1]. Lima Jr J.A, Freire P.T.C, Lima R.J.C, Moreno A.J.D, Filho M, Melo F.E.A, *J. Raman Spectrosc.*, 36 (2005) 1076-1081.
- [2]. Pandirajan S, Umadevi M, Rajaram R.K, Ramakrishnan V, *Spectrochim. Acta A* 62 (2005) 630–636.
- [3]. Silva J.H.da, Lima Jr J.A, Freire P.T.C, Lemos V, Filho J.M, Melo F.E.A, Pizani P.S, Fisher J, Klemke B, Kemner E, Bordallo H.N, *J. Phys.: Condens. Matter*, 21 (2009) 415404.
- [4]. Ebenezar J.D, Ramalingam S, Ramachandra Raja C, Helan V, *J. Theor. Comput. Sci.*, 1 (2013) 1000106.
- [5]. Chandrasekaran J, Ilayabarathi P, Maadeswaran P, *Rasayan J. Chem*, 4 (2011) 320-326.
- [6]. Koetzle T.F, Golict L, Lehmann M.S, Verbist J.J, Hamilton W.C, *J. Chem. Phys.*, 60 (1974) 4690-4696.
- [7]. Parthasarathy R, *Acta Cryst.*, 21 (1966) 422.
- [8]. Krishnan R.S, Sankaranarayanan V.N, Krishnan K, *J. Indian Inst. Sci.* 55 (1973) 66-116.
- [9]. Pawlukoje A, Bobrowicz L, Natkaniec I, Leciejewicz J, *Spectrochim. Acta A*, 51 (1995) 303-308.
- [10]. Paiva F.M, Batista J.C, Rego F.S.C, Lima Jr. J.A, Freire P.T.C, Melo F.E.A, Filho J.M, Menezes A.S. de, Nogueira C.E.S, *J. Mol. Struct.*, 1127 (2017) 419-426.
- [11]. M.J. Frisch et.al., Gaussian 09, Revision A.1, Gaussian Inc., Wallingford CT, 2009.
- [12]. R. Dennington, T. Keith, J. Millam, GaussView 5.0, Semichem Inc., 2009.
- [13]. Gangopadhyay, P. Sharma, R.K. Singh, *Spectrochim. Acta A* 150 (2015) 9–14.
- [14]. M.H. Jamroz, *Spectrochim. Acta A* 114(2013) 220-230.
- [15]. Desiraju G.R, Steiner T, *The Weak Hydrogen Bond*, Oxford University Press, New York, (1999).
- [16]. Bellamy L.J, *The Infrared Spectra of Complex Molecules*, third ed., Chapman and Hall, London, 1975.
- [17]. Colthup N.B, Daly L.H, Wiberley S.E, *Introduction to Infrared and Raman Spectroscopy*, Academic Press Inc, New York and London, 1964.
- [18]. Krishnan R.S, Katiyar R.S, *Bull. Chem. Soc. Japan* 42 (1968) 2098-2101.
- [19]. Dollish F.R, Fateley W.G, Bentley F.F, *Characteristic Raman Frequencies of Organic Compounds*, John Wiley and Sons, Chichester, New York, Brisbane, Toronto, 1974.